

國立交通大學

物理所

碩士論文

多層結構於有機太陽電池的應用

Organic bulk-hetero-junction solar cell

in multilayer structure



研究生：王櫻璇

指導教授：孟心飛 教授

洪勝富 教授

中華民國九十六年六月

多層結構於有機太陽電池的應用

Organic bulk-hetero-junction solar cell in multilayer structure

研究生：王櫻璇

Student：Ying-Hsuan Wang

指導教授：孟心飛

Advisor：Hsin-Fei Meng

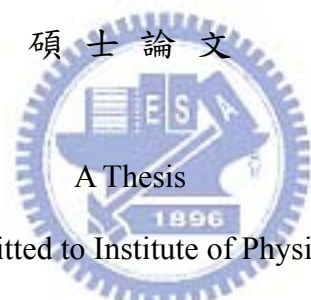
洪勝富

Sheng-Fu Horng

國立交通大學

物理研究所

碩士論文



A Thesis

Submitted to Institute of Physics

College of Science

National Chiao Tung University

in partial Fulfillment of the Requirements

for the Degree of

Master

in

Institute of Physics

June 2007

Hsinchu, Taiwan, Republic of China

中華民國九十六年六月

多層結構於有機太陽電池的應用

國立交通大學物理研究所碩士班

學生：王櫻璇

指導教授：孟心飛教授
洪勝富教授

摘要

隨著能源短缺，除了節約能源，積極開發新的替代能源也越來越趨重要。因此，這篇論文的目標在建立一個太陽電池的模型，從中了解太陽電池的操作及表現，以期進一步改善其效益。在此模型下，以混合有機材料(bulk heterojunction)太陽電池為主體模擬多層結構，藉由多層結構的特性改善太陽電池的效益。

本論文的研究結果包括:

- 1.比較載子移動率(carrier mobility)對元件表現的影響，在此模擬下，發現最佳化的載子移動率大小是 $10^{-3} \text{ cm}^2/\text{Vs}$ 。
- 2.在元件的多層結構中利用阻擋層的特性，藉由減少光電流的損失，來達到提高 short-circuit current (J_{sc})及 fill factor (FF)，證明多層結構的確可提高元件效益。



Organic bulk-hetero-junction solar cell in multilayer structure

Student : Ying-Hsuan Wang

Advisor : Hsin-Fei Meng

Sheng-Fu Horng

Institute of Physics
National Chiao Tung University

ABSTRACT

The thesis represents the bulk heterojunction solar cells in multilayer structure. The cell is of the structure that a mixed donor-accepter layer sandwiched between blocking layers. As the need for renewable energy sources becomes more urgent, photovoltaic energy conversion is attracting more and more attention. Multilayered cells with blocking layers are expected to enhance the efficiency of solar cells by reducing the loss of the photocurrent. In this work we build a model and simulate the bulk heterojunction solar cells in multilayer structure. The efficiency of the cell is enhanced due to that the blocking layers improve the short-circuit current, J_{sc} , and the fill factor (FF). By carefully check and discussion we expect that the increase of J_{sc} and FF is due to the redution the recombination current. The carrier mobility effect in bulk heterojunction cells is also discussed in this work. The optimum carrier mobility is $10^{-3} \text{ cm}^2/\text{Vs}$.

致謝

首先，非常感謝我的指導老師：孟心飛教授在這些日子裡對我的指導。在每一次的討論當中我都學習到很多東西，也因為如此，我才能一步步向前進。能在研究中維持興趣是很開心的感覺，感謝老師讓我在邊作邊學中得到進步，也讓我學習到研究應有的態度，這讓我獲益良多。

我也要感謝理論組的學長姐：紀互學長及宜秀學姊，在做理論研究的過程中，感謝他們的指導，也感謝信榮學長幫助我學會如何去解決問題。也謝謝實驗室的大家在這些日子裡帶來的歡笑聲。

我要非常感謝我的家人及好朋友在這些日子裡對我的支持，因為有你們的陪伴，讓我對這些日子充滿感激，謝謝你們。



目 錄

中文摘要	多層結構於有機太陽電池的應用	i
英文摘要	Organic bulk heterojunction solar cell in multilayer structure	ii
誌謝		iii
目錄		iv
一、	Introduction	1
二、	The device model for BHJ solar cell	3
2.1	Bulk heterojunction solar cell working principle	3
2.2	Factors to decide PCE	4
2.3	MIM model	5
2.4	Basic equations	6
2.5	The device model for BHJ solar cell in multilayer structure	8
三、	Results and discussion	10
3.1	Mobility effect in Bulk heterojunction solar cell with single layer	10
3.2	Blocking layer effect	13
四、	conclusion	19
References		20

Chapter1 Introduction

Organic solar cells base on the bulk heterojunction (BHJ)[1] concept are particularly attractive, mainly due to their potential for low cost, ease of fabrication, and mechanical flexibility. For the polymer solar cells highest efficiencies reaching up to 5% have been reported [2, 3]. However efficiencies of these thin-film organic devices have not yet reached those of their inorganic counterparts (power conversion efficiency~10–20%); the perspective of cheap production (employing, e.g., roll-to-roll processes) drives the development of organic photovoltaic devices further in a dynamic way.

The process of converting light into electric current in an organic solar cell is accomplished by the follow four steps: (i) Absorption of photons, leading to the creation of excitons. (ii) Excitons start to diffuse (iii) Exciton dissociation occurs (iv) The separated free charge carriers transport to the electrodes. The number of created charges that are collected by the electrodes are governed by the fraction of photons absorbed, the fraction of electron-hole pairs that are dissociated, and finally the fraction of separated charges that reach the electrodes. The photogeneration of free charge carriers from the dissociation of electron-hole pairs has been explained by Onsager theory on geminate recombination [4]. Braun has made an important refinement to this theory [5]. Bimolecular recombination in organic semiconductors is known to follow the Langevin expression. Charge transport in the device depends on the continuity equation, Poisson's equation, and drift-diffusion current. According to these theories, a device model for the bulk hetero-junction solar cells is established [6]. The importance of these models is to help us understand the physics in BHJ solar cell. However all these models focus on single layer devices. There is no report about devices in multilayer structure based on metal-insulator-metal (MIM) picture which means that the device is thought to be built up by one semiconductor with the lowest unoccupied molecular orbital (LUMO) of the acceptor and the highest occupied molecular orbital (HOMO) of the donor as valence and conduction band. The MIM model contains drift and diffusion of charge carriers, and the effect of space charge on the electric field in the device. In this article we develop a theoretical model based on Blom et al that enables us to simulate the multilayered devices by tuning the boundary conditions of the devices [7]. Owing to the experiences on multilayered polymer light-emitting diodes (PLED) in our laboratory, we speculate the efficiency of solar cells in multilayer structure may be enhanced.

In a donor/acceptor (D/A) bilayer device, a donor and an acceptor material are stacked together with a planar interface, where the charge separation occurs. The advantage of the

D/A concept lays to a great extent in the relative stability of the charge separated state. Hence, holes and electrons are effectively separated from each other, and thus charge recombination is greatly reduced. However, because the exciton diffusion length for most organic solar cell materials is below 20 nm, only those excitons generated in a region smaller than 20 nm from the interface contribute to the photocurrent. For this reason the thickness of the D/A device are smaller than 40 nm, which is too thin to absorb light sufficiently. Hence the D/A bilayer device is limited because the exciton diffusion length is much shorter than the optical absorption length of the film.

The bulk hetero-junction is to intimately mix the donor and acceptor components in bulk, and it is different from the bilayer device due to it exhibits a largely increased interface area where charge separation occurs and each donor–acceptor interface is within a distance less than the exciton diffusion length of each absorbing site, no loss due to too small exciton diffusion lengths is expected because ideally all excitons will be dissociated within their lifetime. However, the collection efficiency of photo-generated carriers in the bulk heterojunction cell is critically dependent on the transport properties of the interpenetrating network of the donor and acceptor materials.

First, we consider the mobility effect of the bipolar device. Second, we consider a blocking layer between the active layer and the electrode to stop the carriers that diffuse to the opposite sides of their collector region. Forrest et al have presented a cell in hybrid planar-mixed hetero-junction (D/D:A/A) and used the modified diode equations to simulate the experiment results [8]. In this article we focus on the cells contains mixed donor and acceptor in one layer sandwiched between electron blocking layers (EBL) and hole blocking layers (HBL) and then address on charge carrier mobility, multilayer structures (EBL/D:A/HBL). The existence of the blocking layer is to avoid the carrier losses from diffusion to the wrong direction. The multilayer structures we used are in Fig3.4 and Fig3.7, the effect of the blocking layer in these two structure is discussed, In ohmic contact-contact limited device, the V_{oc} is increased due to large electrons are stop by EBL at the voltage near flat band voltage. In bipolar BHJ device, J_{sc} , V_{oc} is increased due to the reduction of the recombination.

This paper is organized as follows: Section II introduces the basic equations to describe the MIM model, Section III represents and discusses the results, and Sec. IV draws the conclusion.

Chapter 2 The device model for BHJ solar cell

2.1 Bulk Heterojunction solar cell working principle

The bulk heterojunction concept is to blend donor-type and acceptor-type materials in one layer (D:A) so that each donor-acceptor interface is within a distance less than the exciton diffusion length of each site.

The energetic diagram of BHJ device is depicted in the Fig. 2.1.

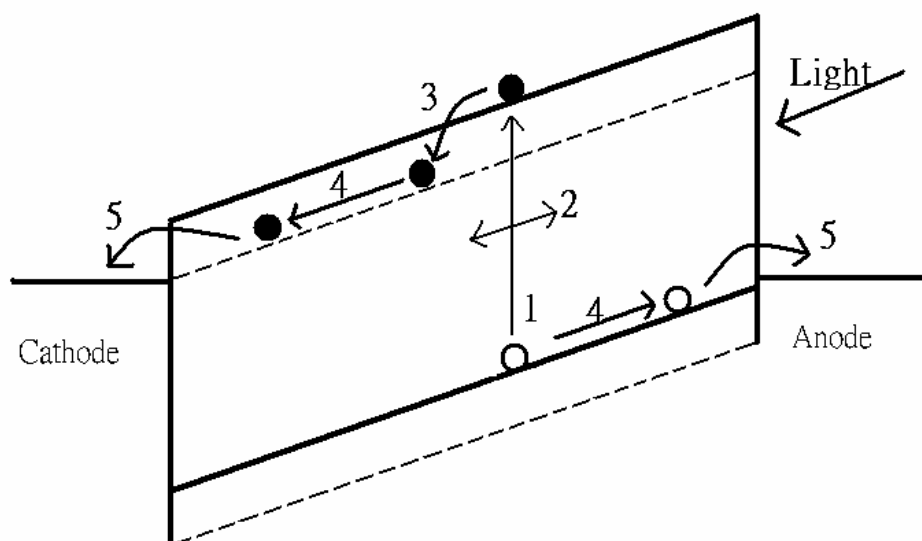


Fig. 2.1: The schematic energy profile of BHJ solar cell. The solid line represents the energy level of donor-type material and the dash line represents the acceptor-type material.

The working principle of BHJ solar cell is divided to five parts as follows:

- (1) Sunlight photons which are absorbed by the donor material, leading to the creation of exciton.
- (2) The created excitons start to diffuse.
- (3) Exciton dissociation takes place leading to the charge separation.
- (4) The separated free charge carriers are transported with the aid of the internal electric field, cause by the use of electrodes with different work functions.
- (5) The free carriers are collected by the electrodes and driven into the external circuit.

At the interface, the resulted potential drop is larger than the exciton binding energy. Hence, the organic D/A interface separates excitons much more efficient than an organic/metal interface in the single layer device.

2.2 Factors to decide PCE

In order to study the efficiency of BHJ solar cell, the current -voltage (I-V) characteristics under illumination are considered, which is shown in Fig. 2.2

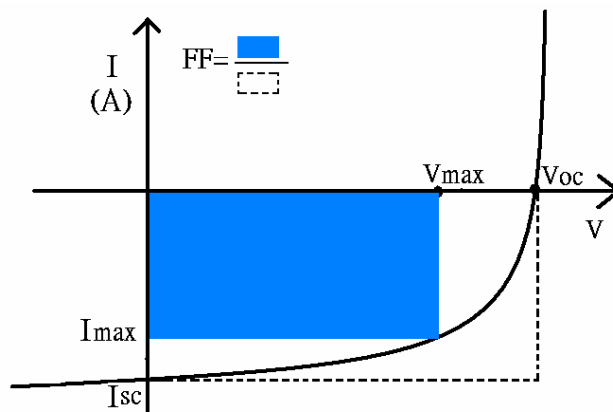


Fig. 2.2: J-V curve of BHJ solar cell under illumination.

The open-circuit voltage, V_{oc} , is the maximum photovoltage that can be generated in the cell and corresponds to the voltage where current under illumination is zero. The maximum current that can run through the cell at zero applied voltage is called the short-circuit current, I_{sc} . The maximum of the obtained electrical power P_{max} is located in the fourth quadrant where the product of current I and voltage V reached its maximum value, the fill factor:

$$FF \equiv \frac{I_{max} \times V_{max}}{I_{sc} \times V_{oc}}$$

The power conversion efficiency (PCE) of a BHJ solar cell:

$$PCE \equiv \frac{P_{max}}{P_{in}} = \frac{I_{sc} \times V_{oc} \times FF}{P_{in}}$$

The essential parameter which determine the power conversion efficiency of thin film solar cell devices are the sort-circuit current (I_{sc}), the open-circuit voltage (V_{oc}), and the fill factor

(FF). Formation of a bulk hetero-junction by mixing the polymer (donor) and the fullerene (acceptor) lead to an enhancement of J_{sc} due to an efficient charge separation. However, it is still much lower than the J_{sc} reported for inorganic devices. This lower photocurrent is mainly due to the spectral mismatch between the sunlight and the absorption spectrum of the polymers used. The performance of BHJ solar cells is known to be critically dependent on the choice of the electrodes. In case of non-ohmic contacts, V_{oc} is determined by the work function difference of the electrodes, and thus follows the metal-insulator-metal (MIM) model. For ohmic contacts the V_{oc} is governed by the LUMO and HOMO levels of the donor and acceptor, respectively, because the electrode work functions become pinned close to the LUMO and HOMO levels of the donor and acceptor. However, for ohmic contacts the accumulated charges at the interface will create a band bending, which leads to a reduction of the electric field in the bulk of the devices and hence influence the V_{oc} of the organic solar cells. The band bending created by accumulated charges at both interfaces due to Ohmic contacts produce a considerable loss in V_{oc} of $\sim 0.38V$ at room temperature [9].

The J_{sc} , V_{oc} and FF also depend on parameters such as: light intensity, temperature, charge carrier mobility, composition of the components, thickness of the active layer, the choice of the electrodes used, as well as the solid state morphology of the film. Their optimization and maximization require a clear understanding of the device operation.

2.3 MIM model

In order to understand the physics behind the BHJ solar cells, a numerical model must to be established. However, different to classical p-n junction cells with spatially separated p-and n-type regions of doped semiconductors, bulk heterojunction cells consist of an intimate mixture of two un-doped (intrinsic) semiconductors. An alternative approach is to use the metal-insulator-metal (MIM) concept, where a homogeneous blend of two semiconductors (donor/acceptor) is described as one semiconductor with properties derived from the two materials. The lowest unoccupied molecular orbital (LUMO) of the acceptor and the highest occupied molecular orbital (HOMO) of the donor act as valence and conduction band of the semiconductor. The energy difference between the LUMO of the acceptor and the HOMO of the donor functions as the effective band gap of the semiconductor.

2.4 Basic equations

An accurate and reliable numerical description of BHJ solar cells is highly desirable when searching for ways to optimize their performance. The metal-insulator-metal (MIM) model used in this thesis is based on an effective medium approach, treating the blend of both components as one intrinsic semiconducting material. Basic equations used to describe the transport properties are the continuity equations, with a drift-diffusion current, couple to Poisson's equation

$$\frac{\partial n}{\partial t} = \frac{1}{q} \frac{\partial J_n}{\partial x} + G - R$$

$$\frac{\partial p}{\partial t} = -\frac{1}{q} \frac{\partial J_p}{\partial x} + G - R$$

$$\frac{\partial E}{\partial x} = \frac{q(p - n)}{\varepsilon}$$

where

$$J_n = q\mu_n \left(nE + \frac{kT}{q} \frac{\partial n}{\partial x} \right)$$

$$J_p = q\mu_p \left(pE - \frac{kT}{q} \frac{\partial p}{\partial x} \right)$$



where $n(p)$ is the electron (hole) density, $J_n (J_p)$ is the electron (hole) current density, G is the free carrier generation rate, R is the bimolecular recombination rate, $\mu_n (\mu_p)$ is the electron (hole) mobility, q is the elementary charge, E is the electric field and ε is the dielectric constant.

In our model, we set electron (hole) mobility constant with the electric field instead of the field dependent mobility. Bimolecular recombination in organic semiconductors is known to follow the Langevin expression, $R = \gamma np$, where the recombination coefficient is given by

$$\gamma = \frac{q}{\langle \varepsilon \rangle} \langle \mu \rangle$$

$\langle \mu \rangle$ is the spatially averaged sum of hole and electron mobilities and $\langle \varepsilon \rangle$ is the spatially averaged dielectric constant.

The rate of generation of bound electron hole pairs is assumed to be homogeneous

throughout the device, and we also set the constant free carrier generation rate with respect to the position in this model.

$G = \text{constant with respect to } x$

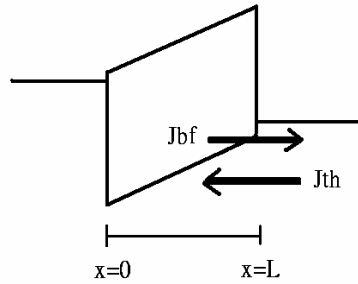
The boundary conditions are given by carrier injection at the boundary $x=0$ and $x=L$. There are thermionic emission and backflow current.

Consider the hole current at $x=L$

$$J_p(L) = -J_{th} + J_{bf}$$

where

$$J_{th} = AT^2 e^{-\phi_b/kT}$$



A is the Richardson constant and ϕ_b is the Schottky barrier height. The back flow current is taken to be proportional to the hole density at the interface

$$J_{bf} = \nu p(L)$$

The kinetic coefficient ν is determined by detailed balance between thermionic and back flow current.

$$\nu = \frac{AT^2}{n_0}$$

And the quasi- equilibrium hole density at the contact $x=L$

$$p(x=L) = n_0 e^{-\phi_b/kT}$$

n_0 is the effective total density of states.

The potential drop over the active layer gives two boundary conditions. At zero applied voltage, the potential drop is equal to the built-in potential, V_{bi} . The built in potential is given by

$$eV_{bi} = \phi_{an} - \phi_{cat}$$

where ϕ_{an} and ϕ_{cat} are work functions for the anode and the cathode, respectively. When an external voltage is applied on the cell, the potential drop becomes

$$\psi(L) - \psi(0) = V_{bi} - V_{appl}$$

where V_{appl} is the applied voltages.

2.5 The device model for BHJ solar cell in multilayer structure

Electrons in the bulk have three ways to transport shown in the Fig. 2.3. One way for electrons to go is to go to the left side, collected by cathode and contribute to photocurrent (1). When the electrons go to the right sides (2) or recombine with holes (3), they contribute nothing but make energy loss. Hence, we treat process 2 and process 3 as the origin of loss of the photocurrent. The multilayered structure contains blocking layers is to avoid the loss that electrons go to the wrong side (process 2).

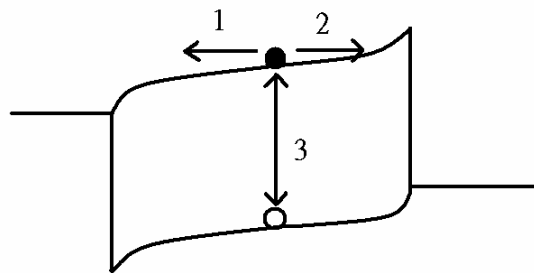


Fig. 2.3: Possible ways for electrons in the bulk.

The schematic energy profile for multilayered BHJ cell is shown in Fig. 2.4. The EBL C stops electrons to diffuse to the anode, and the HBL A stops holes to diffuse to cathode.

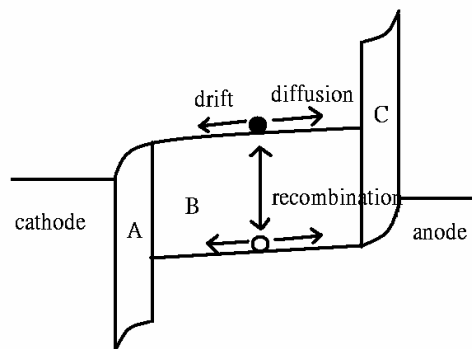


Fig. 2.4: Schematic energy profile for multilayered BHJ cell. Layer A and layer C are carrier blocking layers to stop carriers to go to the wrong side.

We make the approximation based on the single layer model and tune the boundary conditions. The boundary conditions are set that the electron (hole) current and electron (hole) density in the blocking layer C (blocking layer A) are equal to zero.

$$J_n(\text{layerC}) = 0$$

$$n(\text{layerC}) = 0$$

$$J_p(\text{layerA}) = 0$$

$$p(\text{layerA}) = 0$$

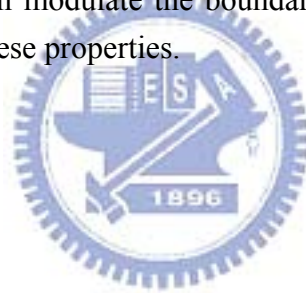
here the function for blocking layer is only to stop carriers to go to the wrong side and absorb no lights, i.e. no photocurrent is contributed by these two layers.

$$G(\text{ layerB }) = \text{constant with respect to position}$$

$$G(\text{ layerC }) = 0$$

$$G(\text{ layerA }) = 0$$

From these restrictions, we can modulate the boundary conditions in our model to simulate the multilayer structure with these properties.



Chapter 3 results and discussion

In this chapter, some device parameters are taken identical: dielectric constant $\epsilon = 3$, $n_0 = 10^{21} \text{ cm}^{-3}$, $G = 3 \times 10^{21} \text{ cm}^{-3} \text{ s}^{-1}$, the thickness (L_{BHJ}) of BHJ is 100nm. And then we keep electron mobility equal to the hole mobility in blocking layer and BHJ.

3.1 Mobility effect in BHJ solar cell with single layer

In this subsection, we consider the bipolar devices shown in Fig. 3.1:

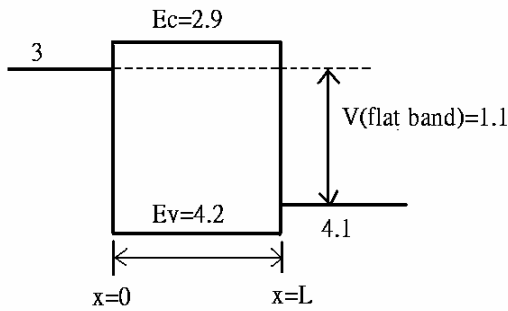


Fig. 3.1: The energy diagram of the single layer BHJ cell.

In BHJ solar cells the recombination follows the Langevin form, controlled by the mobility of the charge carriers.

$$R = \gamma * n * p$$

$$\gamma = \frac{q}{\langle \epsilon \rangle} \langle \mu \rangle$$

As a result, in BHJ cells the mobility simultaneously controls both the carrier extraction and carrier recombination. Recently, the optimum charge carrier mobility in organic solar cells based on annealed P3HT: PCBM devices was reported that $\mu_n = 1.0 \times 10^{-2} - 1.0 \times 10^{-1} \text{ cm}^2/\text{V s}$ for a 10:1 ratio of electron mobility versus hole mobility[10]. It is observed that the efficiency exhibits a distinct maximum as a function of carrier mobility. A low mobility of both carriers will lead to a slower extraction of the charge carriers and hence increase the recombination. In this study, we want to discuss the relationship between carrier mobility and device efficiency in single layer BHJ cells. In our model, we consider a bipolar device with both ohmic contacts, and show

mobilities from $\mu_n = \mu_p = 1.0 \times 10^{-4} \text{--} 1.0 \times 10^{-1} \text{ cm}^2/\text{V s}$. We represent the J-V curve for different mobilities both under illumination and in the dark in Fig. 3.2 and Fig 3.3. Fig 3.3 illustrates that as mobility increase, it gives rise to larger dark current.

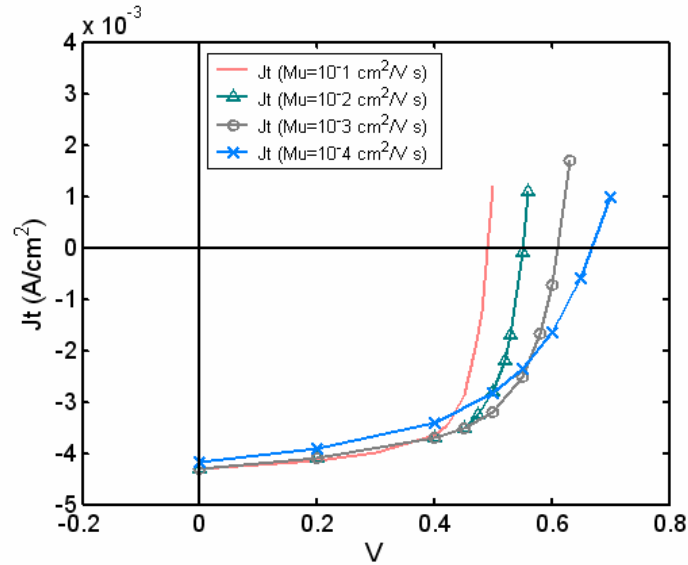


Fig. 3.2: Current density-voltage characteristics (J-V curve) of a BHJ cell in four different mobilities.

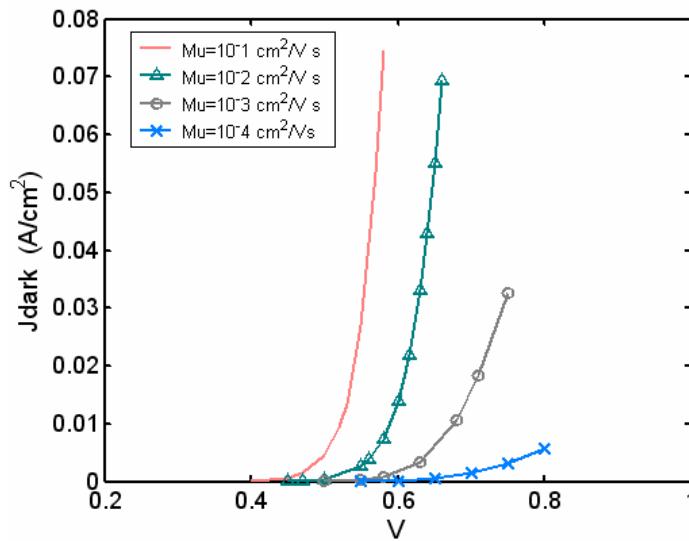


Fig. 3.3: J-V curve of a BHJ cell under dark in four different mobilities.

The results are shown in table I. With the carrier mobility increase the FF increase but the Voc decrease. The FF increase may due to the high mobility helps the carrier collection by the electrode. However the higher carrier mobility increases the

injection of carriers from electrode (dark current) simultaneously. To verify this point we calculate the photocurrent (J_{ph}), which determined by the total current subtract the dark current. First, the Fig. 3.4 shows the potential under illumination is equal to the potential in the dark. Since the injection of carriers from electrode into the bulk see the same potential under illumination and in the dark, we can calculate the photocurrent by $J_{ph}=J_t-J_{dark}$ (J_t : current density under illumination, J_{ph} : photocurrent, J_{dark} : current density in the dark). Fig 3.5 shows the result of photocurrent. The photocurrents of different mobility are almost the same at mobility= 1.0×10^{-3} -- 1.0×10^{-1} $\text{cm}^2/\text{V s}$, therefore it illustrates the reduction of the efficiency at higher mobility indeed is caused by the higher dark current. The optimum mobility here is 10^{-3} cm^2/Vs .

TABLE I. Performance of devices with different mobilities.

	J_{sc} (A/cm^2)	V_{oc} (V)	FF (%)
$\mu = 1.0 \times 10^{-4} \text{cm}^2/\text{V s}$	0.00418	0.66	51
$\mu = 1.0 \times 10^{-3} \text{cm}^2/\text{V s}$	0.0043	0.61	62
$\mu = 1.0 \times 10^{-2} \text{cm}^2/\text{V s}$	0.0043	0.55	67
$\mu = 1.0 \times 10^{-1} \text{cm}^2/\text{V s}$	0.0043	0.49	69

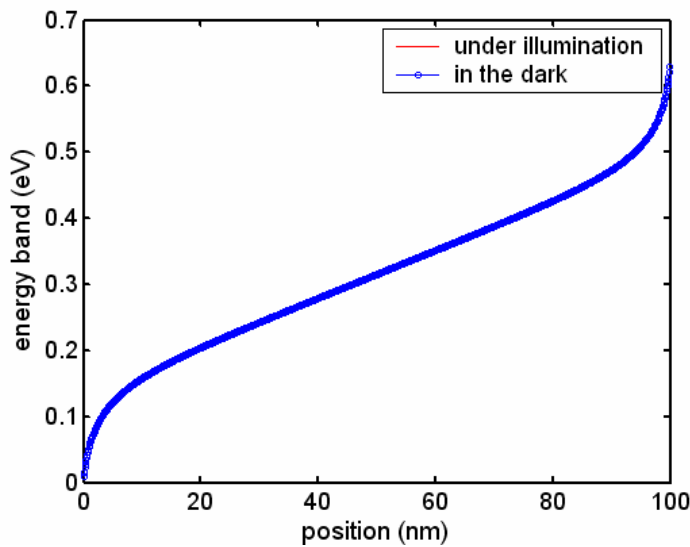


Fig. 3.4: the energy band in the bulk at $V=0.47\text{V}$

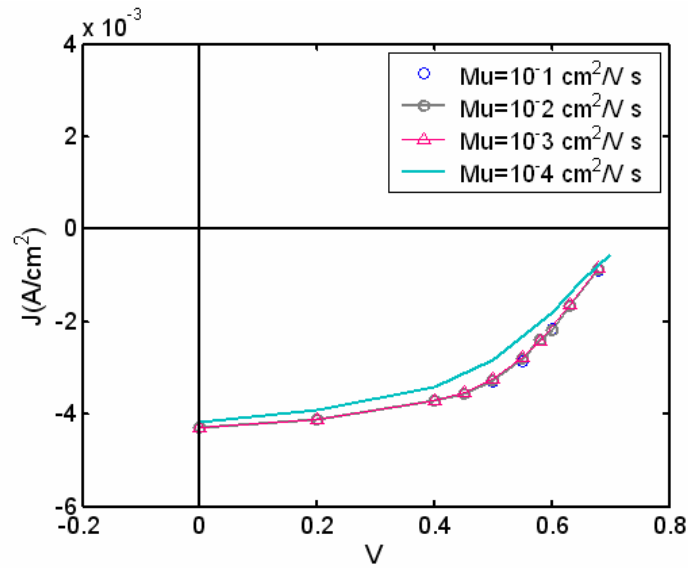


Fig. 3.5: Calculated photocurrent of BHJ cells with different mobility.

3.2 Blocking layer effect

(a) Ohmic contact-contact limited device with EBL

The EBL is to avoid the loss that electrons go to the wrong side (see Fig 2.3 process 2). We develop a device structure that exists an ohmic contact for electron injection and a contact limited for hole to inject. Although the BHJ using both ohmic contacts for carrier injection and extraction, the structure here excludes the hole injection by a high barrier height of hole to simplify the problem, making us to be clear that how EBL affects the electron transport. So we set a structure shown in Fig. 3.6 to verify the EBL effect. The electron (hole) mobility of the BHJ is equal to the EBL, flat band voltage =1.1V, and the boundary condition is described in the Chapter 2.

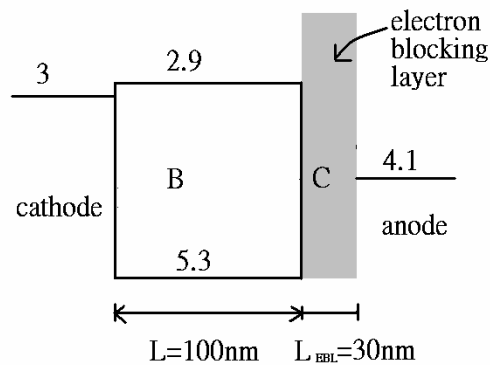


Fig. 3.6: Ohmic contact-contact limited device with EBL.

The electron (hole) mobilities are the same in the layer B and layer C.

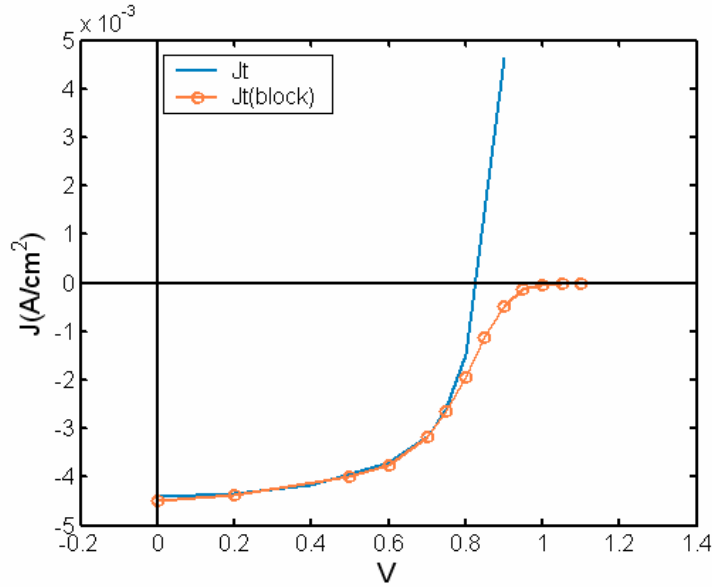


Fig. 3.7: J-V curve of ohmic contact-contact limited device with and without EBL.

Fig. 3.7 shows the result of BHJ cells with and without EBL. At $V=0V - 0.8V$, the behavior of these two current density is almost the same, but at $V > 0.8V$ the current density of the cell with EBL does not become zero until $1V$. At $V=0V-0.8V$, the EBL seems to present no effect which may due to the diffusion current does not play a important role in the voltage range, since electric field in the bulk is large and the extraction of electrons is easy. However at higher voltage near flat band voltage, the diffusion of electrons to the wrong side becomes important because the electric field in the bulk is small, hence the extraction of electron becomes more difficult. The effect of EBL is important now to stop the electrons to be collected by anode. As a result, electrons may diffuse to the right side and be stopped by the EBL, result the accumulation of electrons at the bulk near EBL. Fig. 3.8(a), 3.8(b) represent the electron carrier density vs distance for applied voltage $V=0.9V$. It shows that at $V = 0.9V$, the electrons are indeed stopped by the EBL and hence accumulate near the EBL. The accumulated electrons turn to diffuse to the left side at $x=80\sim 100nm$ and contribute to photocurrent. Because the direction of diffusion current in this region is the same as photocurrent, it can be considered an addition to the photocurrent, and hence increase the V_{oc} . Although the efficiency of ohmic contact-contact limited device seems not to increase, the current remains to higher voltages, which is quite different from the device without EBL.

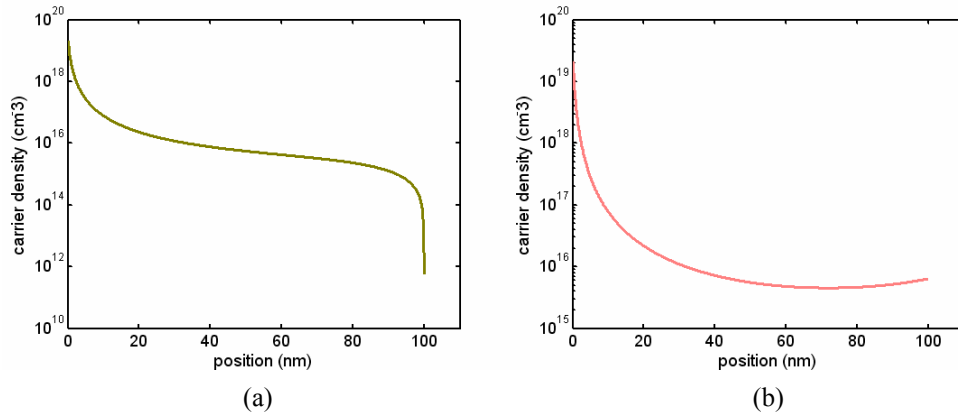


Fig. 3.8: The electron carrier density vs position with blocking layer at $V=0.9$

(a) Single layer: The carrier density still small at 80-100nm

(b) Multilayer: Electrons accumulate at 80-100 nm and even higher than the carrier density in the middle of the bulk.

(b) Bipolar device

After confirming the EBL effect in ohmic contact-contact limited device, we turn to check the blocking effect in the bipolar BHJ cells. The structures of bipolar device with single layer and multilayer are shown in Fig. 3.9, the total device thickness in multilayer $L_t=L_A+L_B+L_C=30+100+30=160$ nm.

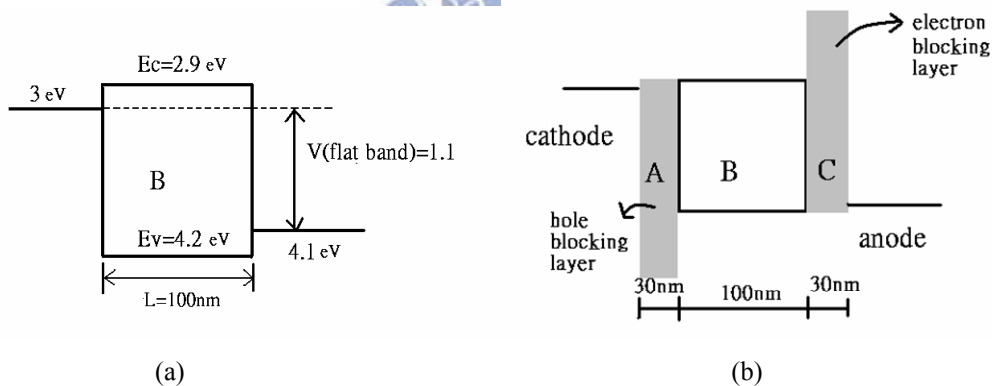


Fig. 3.9: Energy profile for BHJ cells.

(a) without blocking layers

(b) with HBL (Layer A) and EBL (Layer C).

The total device thickness in (a)=100nm, and in (b)=160nm

The mobilities are all set as the same value and two different mobilities are compared. The results of mobility equal to $10^{-3} \text{ cm}^2/\text{V s}$ of BHJ cell with and without carrier blocking layer are shown in Fig. 3.10. Both J_{sc} and FF of the multilayer device with blocking layers are higher than the single layer one. This is different effect from the ohmic contact-contact limited device because we don't see any improvement of J_{sc} and FF in ohmic contact-contact limited device. The reasons of J_{sc} enhancement may due to the reduction of recombination of carriers. Fig. 3.11 shows the recombination in the bulk. The max recombination happens near the side of bulk ($x=5\text{nm}$ and 95nm) due to the large injection from the electrodes and form accumulated charges schematically shown in Fig 3.12 (a). With adding the blocking layers in to the bipolar BHJ, the maximum recombination zone moves into the blocking layers. However in blocking layers there is only one kind of carrier and the carrier recombination in bulk is therefore reduced (Fig 3.12(b)). The direct evidence is shown in Fig. 3.13. The recombination current is actually reduced in the multilayer device. This is quite interesting that the blocking layers can also help to reduce the carrier recombination in the active layer and enhance the J_{sc} and FF. As for the mobility of $10^{-2} \text{ cm}^2/\text{V s}$, J_{sc} and FF are also enhanced compared to the single layer one which is shown in Fig. 3.14. The performance for the single layer and multilayer with $\mu=10^{-3} \text{ cm}^2/\text{V s}$ is in the table II. And the mobility with $\mu=10^{-2} \text{ cm}^2/\text{V s}$ is in the table III.

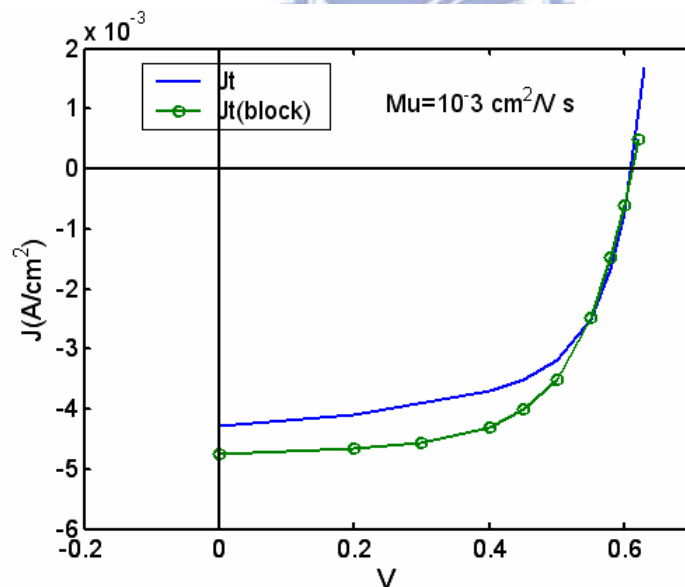


Fig. 3.10: Show the J-V curve with mobility= $10^{-3} \text{ cm}^2/\text{V s}$ in the single layer (J_t) and in the multilayer ($J_t(\text{block})$).

Table II

$\mu = 10^{-3} (\text{cm}^2/\text{V s})$	V_{oc} (V)	J_{sc} (A/cm^2)	FF (%)
Single layer	0.61	0.0043	62
With blocking layer	0.61	0.0047	62.6

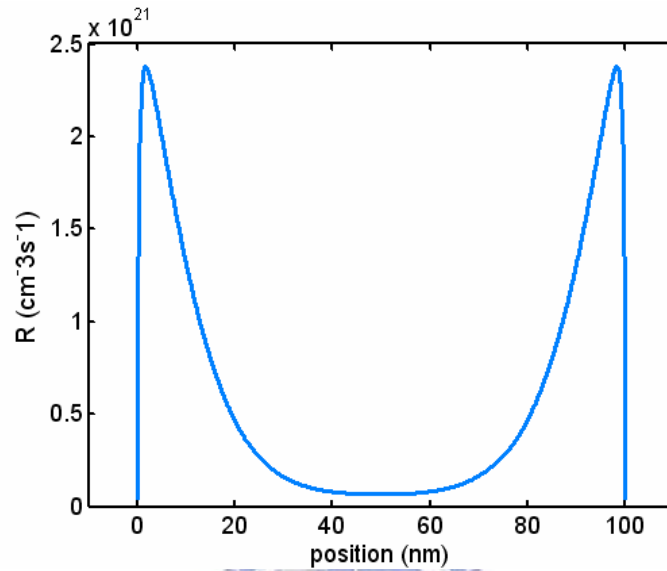


Fig. 3.11: The recombination vs position with a single layer in the bipolar BHJ devices

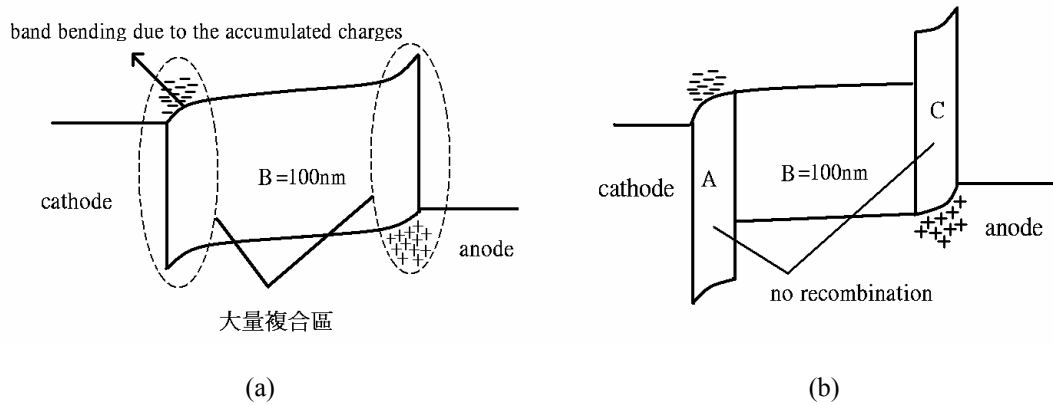


Fig. 3.12: Show the recombination rate between the single layer and multilayer.

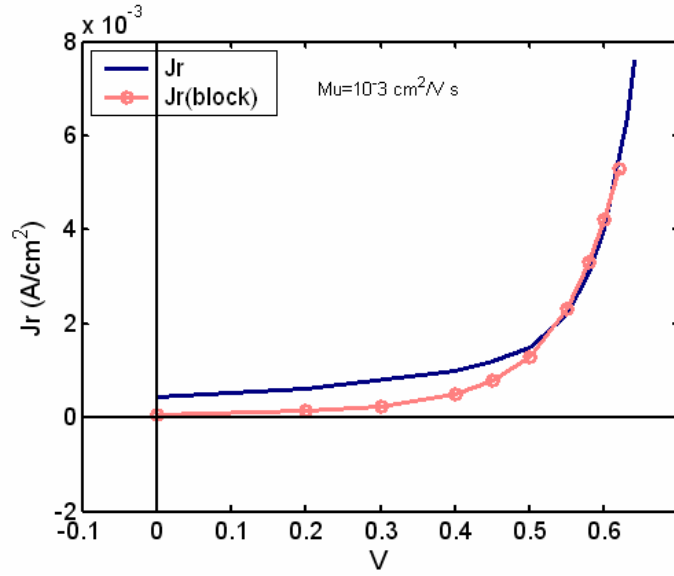


Fig. 3.13: Recombination current J_r vs V as a function of single layer(J_r) and multilayer ($J_r(\text{block})$)

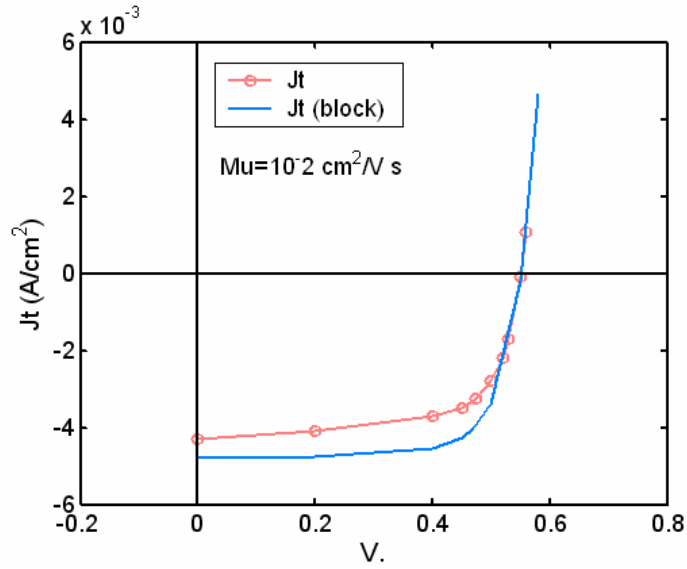


Fig. 3.14: Show the J-V curve with mobility= $10^{-2} \text{ cm}^2/\text{V s}$ in the single layer (J_t) and in the multilayer ($J_t(\text{block})$).

Table III

$\mu = 10^{-2} (\text{cm}^2/\text{V s})$	V_{oc} (V)	J_{sc} (A/cm ²)	FF (%)
Single layer	0.55	0.0043	67
With blocking layer	0.55	0.0048	73

Chapter 4 Conclusion

In conclusion we have show the mobility effect in the single layer BHJ device. When mobility is higher than the optimum value(here is $10^{-3} \text{ cm}^2/\text{V s}$), we get the lower efficiency, the effect is due to the large dark current injection when the mobility is high in the BHJ device.

The result of the blocking layer in BHJ device is represented. In ohmic contact-contact-limited device, the V_{oc} is increased due to large electrons are stop by EBL at the voltage near flat band voltage, in bipolar BHJ device, J_{sc} , V_{oc} is increased due to the reduction of the recombination.



References

- [1] G. Yu, J. Gao, J.C. Hummelen, F. Wudl, and A.J. Heeger, *Science* **270**, 1789 (1995).
- [2] G. Li, V. Shrotriya, J. Huang, Y. Yao, T. Moriarty, K. Emery, and Y. Yang, *Nat. Mater.* **4**, 864 (2005)
- [3] W. L. Ma, C. Y. Yang, X. Gong, K. Lee, and A. J. Heeger, *Adv. Funct. Mater.* **15**, 1617 (2005)
- [4] L. Onsager, *Phys. Rev.* **54**, 554 (1938)
- [5] C. L. Braun, *J. Chem.* **2**, 599 (1984)
- [6] L. J. A. Koster, E. C. P. Smits, V. D. Mihailetschi, and P. W. M. Blom, *Phys. Rev. B.* **72**, 085205 (2005)
- [7] L. J. A. Koster, E. C. P. Smits, V. D. Mihailetschi, and P. W. M. Blom, *Phys. Rev. B.* **72**, 085205 (2005).
- [8] Jiangeng Xue, Soichi Uchida, Barry P. Rand, and Stephen R. Forrest, *Appl. Phys. Lett.* **85**, 5757 (2004)
- [9] V. D. Mihailetschi, P. W. M. Blom, J. C. Hummelen, and M.T. Rispens, *J. Appl. Phys.* **82**, 12 (1997)
- [10] M. M. Mandoc, L. J. A. Koster and P.W.M. Blom, *Appl. Phys. Lett.* **90**, 133504 (2007)

